MINI-RF OBSERVATIONS OF MARE EJECTA EMPLACEMENT DIVERSITY. A. M. Stickle[1], G. W. Patterson[1], D. B. J. Bussey[1], J. T. S. Cahill[1], and the Mini-RF Team, [1]Johns Hopkins University Applied Physics Laboratory, Laurel, MD (angela.stickle@jhuapl.edu).

Introduction: Impact cratering is a primary weathering process of airless bodies and is the dominant method of redistributing material across the lunar surface [1]. Crater ejecta blankets are a window into the impact cratering process and can provide important information regarding the properties of subsurface materials. Radar scattering information, in particular the circular polarization ratio (CPR) [e.g., 2], provides a useful means of investigating these properties. Here, we examine the CPR characteristics of 22 craters that are relatively young and located within nearside Mare deposits (Figure 1). We observe significant diversity in average CPR profiles as a function of crater radius and propose that much of this diversity is an expression of subsurface layering excavated during the impact process.

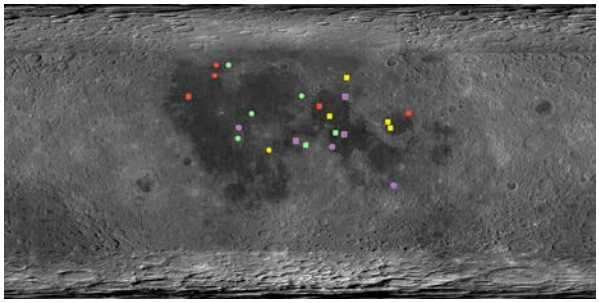

Figure 1. LROC WAC mosaic showing the locations of the 22 young, fresh mare craters studied here. Squares show craters with visible layering structures in the craters walls as identified by Sharpton (2014) [3]. Colors represent general categories of profile shape.

Background: The Miniature Radio Frequency (Mini-RF) instrument flown on NASA's Lunar Reconnaissance Orbiter (LRO) is a Synthetic Aperture Radar (SAR) with a hybrid dual-polarimetric architecture. I.e., the radar transmits a circularly polarized signal, and receives orthogonal linear polarizations and their relative phase [4]. The returned information can be represented using the classical Stokes parameters (S_1, S_2, S_3, S_4) [5], which can be used to derive a variety of useful products to characterize the radar scattering properties of the lunar surface. CPR is commonly used in analyses of planetary radar data [6-7] and is given by: CPR = $(S_1-S_4)/(S_1+S_4)$. It is a representation of surface roughness on the order of the radar wavelength (e.g., meter scale features).

We have examined the radar scattering properties of the ejecta blankets for 22 young, fresh, mare craters with diameters ranging from 2–55 km, 15 of which have visible layering within the crater walls (Figure 1). Average profiles of the Stokes parameters (S_1 and S_4), and CPR have been calculated as a function of radius for each crater, beginning at the crater rim and extending outward for 100–200 km (approx. 7-10 crater radii). For some of the craters, radial profiles were taken as an average over a select azimuthal range. This is especially useful for examining asymmetries in ejecta blankets due to oblique impacts or anomalous signals due to topography.

Observations and Analysis: Comparing scattering properties as a function of radius reveals information about ejecta emplacement in mare craters. Some commonalities in the scattering profiles are observed for all crater diameters: higher CPR values occur near the crater rim, which decay with radial distance outward, larger craters have a higher CPR than smaller craters, and the overall shapes of the profiles are similar.

When distance from the crater rim is normalized to crater radius (Fig. 2), however, these trends are not as obvious. The overall size progression is still apparent and larger craters have higher CPR near the rim. However, the profile shapes are no longer similar across the size range, and a high CPR "shelf" near the rim is prominently observed for some craters within a region of high CPR extending out to ~0.5 R_c before the signal transitions to the lunar background value. Gambart A and Harpalus E, however, do not follow this trend. A laterally extensive region of high CPR is not observed at Gambart A, where CPR begins to decrease immediately outside the crater. These observations are contrary to what would be expected from optical images, where there is a large, optically bright ejecta blanket around the crater. In contrast, the CPR is high near the rim of Harpalus E and the surface remains rough (with moderate to high CPR values) out to several crater radii from the rim, unlike other area craters. It is possible that age may account for these differences in profile shape. Although all these craters are Copernican, perhaps crater degradation is more apparent in the roughness of the surface than in optical images.

Figure 2 also compares CPR profiles to crater size. With the exception of Petavius B, all the mare craters > 20 km have similar scattering profiles, though different in magnitude. The CPR drops rapidly near the crater rim, but then plateaus for a short distance before dropping again to the lunar background level. These plateaus neither begin nor end at the same relative radius from the crater rim and exhibit significant variations

from the expected CPR characteristics of crater ejecta. We use these data to infer the presence of subsurface layers that, when ejected onto the surface, have different scattering characteristics than surrounding material. The mechanical property differences between layers could result in more blocks on the order of the radar wavelength to be emplaced on the surface, causing a shelf in the CPR profile. This hypothesis is consistent with preliminary M^3 observations [8] that show differing compositions of material being ejected in these craters.

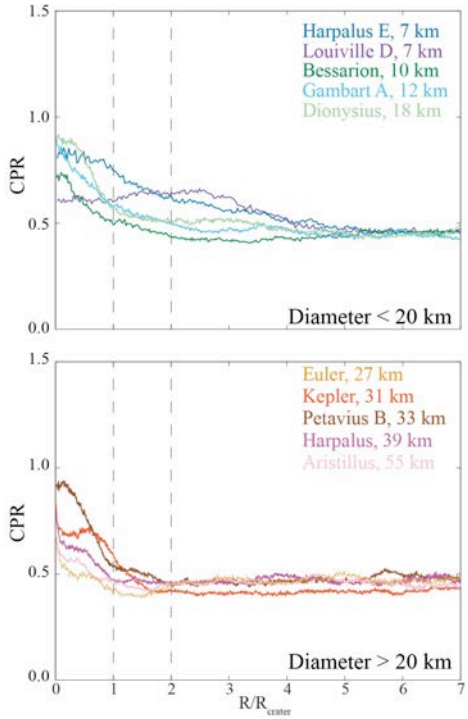

Figure 2. Profiles of average CPR as a function of normalized distance from the crater rim. (top) Mare craters with diameters less than 20 km. (bottom) Mare craters with diameters > 20 km.

These observations reveal that CPR profiles observed adjacent to craters (e.g., Kepler crater) may provide insight regarding subsurface layering in mare regions. Hörz *et al.* [9] estimate that the dominant source depth for primary ejecta within the continuous ejecta blanket is <0.01 times the crater diameter. To a first order, the depth from which material in the continuous ejecta blanket (within approximately 1 crater radius from the rim [10]) is excavated at Kepler crater would then be approximately 300 m, consistent with the approximate depth of the layering observed in LROC NAC images (Fig. 3 top). Thus the CPR profile from Kepler crater may be revealing a discrete subsurface layer that was emplaced at the surface during the impact process.

These observations are consistent for craters with visible layering in the walls studied here. For craters with capping layers (e.g., Bessarion (Fig. 3 bottom) and Dionysius, where the mechanically different layer is seen at the top of the crater wall), the CPR plateaus tend to be at the crater rim, and extend outward a short distance. These high CPR plateaus may be due to the capping layer fragmenting differently than material beneath it, or to the presence of impact melt at the crater rim [e.g., 11]; further detailed analysis will help distinguish these two processes. In contrast, if discrete layers are seen farther down the walls in NAC images (e.g., Kepler), the signal in the CPR appears outward from the crater rim. If no layering is visible in the crater walls (e.g., Gambart A), no shelf is seen in the CPR. Using layer depth estimates with CPR profiles as a function of distance, it may be possible to generate a model for excavation depth of ejecta emplaced on the surface.

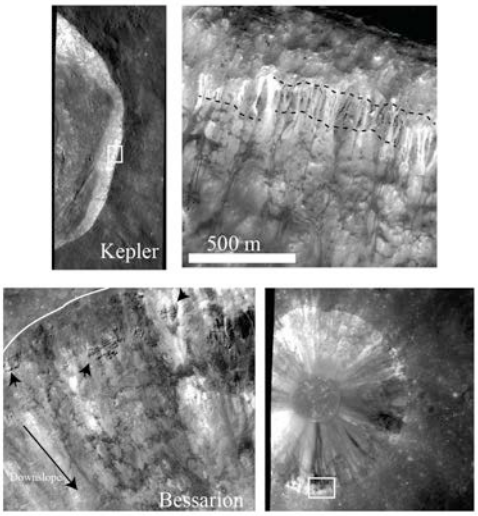

Figure 3. (top, left) LROC NAC mosaic of Kepler Crater (31 km); (top, right) NAC image of layering in the wall of Kepler crater. Dotted lines show approximate edges of subsurface layers observed behind landslides. (bottom, left) NAC image of capping layers in the wall of Bessarion crater, indicated by white box in the NAC mosaic (bottom right).

References: [1] Melosh, H. J. (1989), Oxford Univ. Press; [2] Campbell et al. (2010), *Icarus*, 208, 565-573; [3] Sharpton, V.L. (2014) *JGR-P 119*, 1-15; [4] Raney, R. K. et al. (2011), *Proc. of the IEEE*, 99, 808-823; [5] Stokes (1852), Trans. of the Cambridge Phil. Soc. 9, 399; [6] Campbell et al. (2010), *Icarus*, 208, 565-573; [7] Carter et al. (2012), JGR, 117, E00H09; [8] R. Klima, personal communication; [9] Hörz, F. et al. (1983) *Rev. Geophys. and Space. Phys.*, 21, 1667-1725; [10] Moore et al. 1974, *Proc. 5th LPSC,* 71-100; [11] Neish et al. (2014), *Icarus 239*, 10-117.